INTERNATIONAL JOURNAL OF CLIMATOLOGY, VOL. 13, 347–370 (1993) 551.513.1:551.588.6(71)

CLASS—A CANADIAN LAND SURFACE SCHEME FOR GCMS, II. VEGETATION MODEL AND COUPLED RUNS

D. L. VERSEGHY, N. A. McFARLANE AND M. LAZARE
Canadian Climate Centre, 4905 Dufferin Street, Downsview, Ontario M3H 5T4, Canada

Received 3 April 1992
Accepted 28 July 1992

ABSTRACT

In the companion to the present paper, the soil model associated with CLASS (Canadian Land Surface Scheme) was outlined. In this paper, the accompanying vegetation model is described. This model includes physically based treatment of energy and moisture fluxes from the canopy as well as radiation and precipitation cascades through it, and incorporates explicit thermal separation of the vegetation from the underlying ground. Seasonal variations of canopy parameters are accounted for. The morphological characteristics of the 'composite canopy' associated with each grid square are calculated as weighted averages over the vegetation types present. Each grid square is divided into a maximum of four separate subareas: bare soil, snow-covered, vegetation-covered, and snow-and-vegetation covered.

Test runs were done in coupled mode with the Canadian Climate Centre GCM, to evaluate the performance of CLASS compared with that of the simpler land surface scheme previously used. Two versions of CLASS were run: one with ponded surface water saved between time steps, and one with it discarded. For the seasons of June–July–August and December–January–February, diagnostic calculations showed that the old scheme underestimated the globally averaged land surface screen temperature by as much as 3·0°C, and overestimated the globally averaged precipitation rate over land by up to 1·0 mm day^{-1}. CLASS, on the other hand, produced screen temperature anomalies, varying in sign, of 0·2–0.3°C, and positive precipitation anomalies of 0·6–0·7 mm day^{-1}. The relatively poor performance of the old model was attributed to its neglect of vegetation stomatal resistance, its assumption that the contents of the soil moisture 'bucket' had to be completely frozen before the surface temperature could fall below 0°C, and its use of the force-restore method for soil temperatures, which systematically neglects long-term thermal forcing from the soil substrate. The assumption made in most GCMs that excess surface water immediately becomes overland runoff is shown to result in substantial overestimates of surface screen temperatures in continental interiors.

KEY WORDS Land surface processes General circulation models Canadian land surface scheme Climate modelling

1. INTRODUCTION

In the companion to the present paper (Verseghy, 1991), the soil model associated with CLASS (Canadian Land Surface Scheme) was described, and was shown to simulate a more physically realistic soil thermal and hydrological regime than the model that had been used to date in the Canadian Climate Centre GCM (incorporating the force-restore method for the calculation of soil temperatures and the so-called 'bucket' model for soil moisture). In this paper, the treatment of vegetation in CLASS is outlined, and the performance of the complete model is evaluated.

Vegetation canopies have been shown to exert a profound influence on surface fluxes of heat and moisture. The effects of canopy interception on surface evaporation rates, stomatal resistance on transpiration rates, and rooting depth on the supply of soil moisture available for transpiration were demonstrated by Warrilow *et al.* (1986). The last two are recognized as being particularly important; for example, Meehl and Washington (1988) showed that the sensitivity of soil moisture to climate change in doubled-CO_2 experiments was largely controlled by the amount of soil moisture present in the control run. Improvements in the simulation of certain aspects of land surface climate have been noted when more physically realistic land surface schemes are coupled to GCMs (e.g. Sato *et al.*, 1989; Sud *et al.*, 1990).

0899–8418/93/040347–24$17.00

Finally, the visible and total canopy transmissivities for partly cloudy skies are approximated using equations analogous to (6):

$$\tau_c = \frac{\tau_{c,\odot} K_{\downarrow D} + \tau_{c,\otimes} K_{\downarrow d}}{K_{\downarrow D} + K_{\downarrow d}} \tag{16}$$

$$\tau_{c,VIS} = \frac{\tau_{c,\odot,VIS} K_{\downarrow D} + \tau_{c,\otimes,VIS} K_{\downarrow d}}{K_{\downarrow D} + K_{\downarrow d}} \tag{17}$$

The near-infrared canopy transmissivity can then be obtained using an equation analogous to (11) and (15).

Having obtained the visible and near-infrared canopy albedos and transmissivities, the net shortwave radiation totals $K_{*,c}$ for the canopy and $K_{*,g/s}$ the underlying ground or snow cover can be calculated as:

$$K_{*,g/s} = \hat{\tau}_{c,VIS} K_{\downarrow VIS}[1-\alpha_{g/s,VIS}] + \hat{\tau}_{c,NIR} K_{\downarrow NIR}[1-\alpha_{g/s,NIR}] \tag{18}$$

$$K_{*,c} = K_{\downarrow VIS}[1-\hat{\alpha}_{c,VIS}] + K_{\downarrow NIR}[1-\hat{\alpha}_{c,NIR}] - K_{*,g/s} \tag{19}$$

where the carets denote 'composite canopy' values, calculated as weighted averages over the four major vegetation groups, and $\alpha_{g/s,VIS}$ and $\alpha_{g/s,NIR}$ are the soil or snow visible and near-infrared albedos respectively. Soil albedos are obtained from the all-wave ground albedo α_g (defined in equation (9) of Verseghy, 1991) by making use of the observation that for most soils, $\alpha_{g,NIR} \cong 2{\cdot}0\,\alpha_{g,VIS}$. Snow albedos are calculated as in equations (32) and (33) of Verseghy (1991), with visible albedos of 0·95, 0·84 and 0·61 and near-infrared albedos of 0·72, 0·56 and 0·38 as the boundary values for fresh snow, old dry snow and old melting snow respectively.

The net longwave radiation amounts absorbed by the canopy and the underlying surface, $L_{*,c}$ and $L_{*,g/s}$ respectively, are modelled more simply. A sky view factor χ, describing the degree of canopy closure, is defined as the fraction of sky that the ground underlying the canopy sees. According to studies reported in the literature, the following relations can be defined for the four main canopy types:

$$\chi = \exp(-0{\cdot}5\Lambda) \quad \text{(needleleaf trees)} \tag{20a}$$

$$\chi = \exp(-1{\cdot}5\Lambda) \quad \text{(broadleaf trees)} \tag{20b}$$

$$\chi = \exp(-0{\cdot}8\Lambda) \quad \text{(crops and grass)} \tag{20c}$$

Equations for $L_{*,c}$ and $L_{*,g/s}$ can therefore be written as:

$$L_{*,g} = (1-\hat{\chi})\sigma\bar{T}_c^4 + \hat{\chi}L_{\downarrow} - \sigma T(0)^4 \tag{21}$$

$$L_{*,c} = (1-\hat{\chi})(L_{\downarrow} + \sigma T(0)^4 - 2\sigma\bar{T}_c^4) \tag{22}$$

where $\hat{\chi}$ is the 'composite canopy' sky view factor averaged over the four major vegetation groups, $L_{\downarrow}$ is the incoming atmospheric longwave radiation, $\bar{T}_c$ is the effective canopy temperature and $T(0)$ is the temperature of the underlying ground. The canopy is modelled as behaving like a black body because the complex orientation of leaves in most vegetation stands can be assumed to lead to a high degree of radiation trapping and therefore to an effective emissivity of unity.

2.2. Sensible and latent heat fluxes

Energy fluxes from the canopy to the boundary layer are modelled using the bulk aerodynamic approach. The sensible heat flux from the canopy is written as

$$Q_{H,c} = \rho_a c_P (T_a - \bar{T}_c)/r_a \tag{23}$$

where ρ_a, c_P and T_a represent the density, specific heat and temperature respectively of the air above the vegetation, and r_a is the aerodynamic resistance. The latter is calculated from the surface drag coefficient C_D and the wind speed V_a above the canopy as

$$r_a = [C_D V_a]^{-1} \tag{24}$$

ground below it and the air above it, but remarks that the calculation is not sensitive to the magnitudes of the three weighting factors.)

The latent heat flux from the canopy is calculated using an equation analogous to that for sensible heat. If the canopy surfaces are covered with a film of intercepted precipitation (or if the vapour flux is toward the canopy), evaporation (sublimation) takes place at the potential rate:

$$Q_{E,c,wet}=\frac{L_v\rho_a[q_a-q_{sat}(\bar{T}_c)]}{r_a} \tag{32}$$

where L_v is the latent heat of vaporization of water and $q_{sat}(\bar{T}_c)$ is the saturation specific humidity at $\bar{T}_c$. If the canopy is dry, a resistance r_c must be incorporated into the denominator of (32), to account for the bulk stomatal resistance of the canopy leaves to transpiration:

$$Q_{E,c,dry}=\frac{L_v\rho_a[q_a-q_{sat}(\bar{T}_c)]}{r_a+r_c} \tag{33}$$

Dense, green, unstressed canopies are generally found to have similar, low values of stomatal resistance, ranging from 25 to 100 s m^{-1}. A reasonable representative value for this minimum resistance $r_{c,min}$ is 50 s m^{-1} (Sherratt and Wheater, 1984). If the canopy is incomplete or immature, the resistance is greater. Making use of the assumption that leaf resistances act in parallel, i.e. $1/r_c(\Lambda)=\Lambda/r_l$, where r_l is the stomatal resistance of a single leaf, it can readily be deduced that if $\Lambda<\Lambda_{max}$ for a given canopy type, its unstressed canopy resistance can be obtained as

$$r_c(\Lambda)=r_{c,min}[\Lambda_{max}/\Lambda] \tag{34}$$

Various environmental factors may act upon the canopy to produce stress and cause the stomata to close to prevent excessive transpiration, thus leading to an increase in r_c. The most important of these factors are the incoming solar radiation $K_\downarrow$, the air vapour pressure deficit Δe, the leaf water potential ψ_l, and the canopy temperature $\bar{T}_c$. Most researchers assume the effects of these to be multiplicative. Variations in ψ_l are difficult to model, as they depend on poorly understood aspects of plant physiology; therefore, like many other models, CLASS uses the soil moisture suction $\psi_{s,r}$ in the rooting zone as a surrogate for ψ_l (since the former is in fact the most important factor influencing the latter). Also, to avoid the risk of runaway feedback effects, T_a is used in the calculation of r_c as a surrogate for $\bar{T}_c$. Thus,

$$r_c=\hat{r}_c f_1(K_\downarrow)f_2(\Delta e)f_3(\psi_{s,r})f_4(T_a) \tag{35}$$

where $\hat{r}_c$ is the composite canopy value, averaged over the four major vegetation groups, of the unstressed canopy resistance calculated using equation (34). No data set exists that reports the simultaneous variation of r_c with respect to all of the above parameters, even for one vegetation type. There is also little agreement as to what form the functional dependence should take (e.g. Federer, 1979; Avissar *et al*, 1985; Simpson *et al.*, 1985; Stewart, 1988). This is still an area of ongoing research in the continuing development of CLASS. At present, the following simple relations are used:

$$f_1(K_\downarrow)=\max(1{\cdot}0,\ 500{\cdot}0/K_\downarrow-1{\cdot}5) \qquad (K_\downarrow \text{ in W m}^{-2}) \tag{36a}$$

$$f_2(\Delta e)=\max(1{\cdot}0,\ \Delta e/5{\cdot}0) \qquad (\Delta e \text{ in mbar}) \tag{36b}$$

$$f_3(\psi_{s,r})=\max(1{\cdot}0,\ \psi_{s,r}/40{\cdot}0) \qquad (\psi_{s,r} \text{ in m}) \tag{36c}$$

$$\left.\begin{aligned} f_4(T_a)&=1{\cdot}0, && 40^\circ\text{C}>T_a>0^\circ\text{C}\\ &=5000{\cdot}0/\hat{r}_c, && T_a\geqslant 40^\circ\text{C or } T_a\leqslant 0^\circ\text{C}\end{aligned}\right\} \tag{36d}$$

The value used for $\psi_{s,r}$ is the minimum value of soil moisture suction found for the soil layers contained within the rooting zone; this follows the approach of Radcliffe *et al.* (1980), who assume that plants optimize their energy expenditures by extracting water preferentially from the soil layer with the lowest energy level.

$$E_s=\frac{Q_{E,c}X_s}{L_vX_1+L_sX_s} \tag{43}$$

When the moisture stored on the canopy has been exhausted, transpired water is removed from the soil. The rate of water extraction from each soil layer i in the rooting zone, $E_{T,i}$, is calculated using a weighting function $F_{r,i}$ defined on the basis of the fractional volume of roots R_i and the soil moisture suction $\psi_{s,i}$ in that layer:

$$F_{r,i}=\frac{R_i[\psi_{max}-\psi_i]}{\sum_{i=1}^{N} R_i[\psi_{max}-\psi_i]} \tag{44}$$

where $\psi_i=\min(\psi_{max}, \psi_{s,i})$, ψ_{max} is the critical soil moisture suction at which transpiration effectively ceases (taken to be 150 m), and N is the number of soil layers in the rooting zone. To obtain R_i, a function $R(z)$ is defined as the fractional root volume below a given depth z. The consensus in the literature is that $R(z)$ is usually exponential in form:

$$R(z)=a_1e^{-a_2z}+a_3 \tag{45}$$

where a_1, a_2, and a_3 are constants. According to Feddes *et al.* (1974), for many varieties of crops, grasses and trees, $a_2\cong 3{\cdot}0$. Making use of the boundary conditions $R(0)=1$ and $R(\hat{z}_r)=0$, where $\hat{z}_r$ is the averaged, composite canopy rooting depth, equation (45) becomes

$$R(z)=\frac{\exp(-3{\cdot}0z)-\exp(-3{\cdot}0\hat{z}_r)}{1-\exp(-3{\cdot}0\hat{z}_r)} \tag{46}$$

R_i is then calculated from $R(z)$ as

$$R_i=R(z_{i-1})-R(z_i) \tag{47}$$

where z_{i-1} and z_i are the depths of the top and bottom of the soil layer respectively (see Figure 1 in Verseghy, 1991). Finally, $E_{T,i}$ can be calculated (in m^3 water per m^3 soil) as:

$$E_{T,i}=\frac{Q_{E,c}F_{r,i}}{\rho_wL_v\Delta z_i} \tag{48}$$

where ρ_w is the density of water and Δz_i is the thickness of the soil layer.

2.4. Canopy and ground temperatures

The canopy and ground surface temperatures are calculated by iterative solution of the respective energy balance equations, which are expressed as non-linear functions of $\bar{T}_c$ and $T(0)$ alone. The energy balance equations for the surface under the canopy and for the canopy itself are written as

$$K_{*,g/s}+L_{*,g/s}+Q_{H,g/s}+Q_{E,g/s}=G_o \tag{49}$$

$$K_{*,c}+L_{*,c}+Q_{H,c}-Q_{H,g/s}+Q_{E,c}+S_c=\frac{C_c}{\Delta t}[\bar{T}_c(t)-\bar{T}_c(t-1)] \tag{50}$$

All of the variables on the left-hand sides have been defined in the above sections except for two: S_c is a source (or sink) term for freezing or thawing of moisture stored on the canopy, re-evaluated within each iteration, and G_o is the heat flux into the ground, obtained from equation (16) in Verseghy (1991). The variable C_c represents the heat capacity of the canopy in J m^{-2} K^{-1}, and is calculated as

$$C_c=c_c\hat{W}_c+c_wW_1+c_sW_s \tag{51}$$

where the c terms are the specific heats of vegetation, water and snow respectively, and $\hat{W}_c$ is the standing mass of the composite canopy. The variable c_c is assigned a value of $2{\cdot}7\times10^3$ J kg^{-1} K^{-1}, and $\hat{W}_c$ is

where z_s is the snow depth. The values of $z_{0,M}$ and d are recalculated at each time step from the current values of H.

The standing mass W_c of each of the four canopy groups is assigned a maximum value for each grid square. For trees, W_c is always equal to $W_{c,max}$; leaf fall is assumed to cause a negligible change in canopy mass. For crops and grass, W_c is modified, making use of the instantaneous value of H, to account for growth stage and the burying of vegetation by snow:

$$W_c = W_{c,max} \qquad \text{(trees)} \tag{57a}$$

$$W_c = W_{c,max} H/H_{max} \qquad \text{(crops and grass)} \tag{57b}$$

The vegetation rooting depth z_r is not affected by snow cover, and therefore remains at its maximum value for trees and grass over each grid square. For crops, it is corrected for growth stage:

$$z_r = z_{r,max} \qquad \text{(trees and grass)} \tag{58a}$$

$$z_r = \gamma z_{r,max} \qquad \text{(crops)} \tag{58b}$$

Leaf area index varies seasonally between maximum and minimum values, determined separately for each vegetation type. As in the above calculations, the presence of snow cover does not affect the calculated value of Λ for trees; a correction similar to that for the calculation of W_c is made for crops and grass. (It is assumed for the latter two vegetation types that leaves are distributed approximately uniformly with height.) Thus,

$$\Lambda = \Lambda_{min} + \gamma[\Lambda_{max} - \Lambda_{min}] \qquad \text{(trees)} \tag{59a}$$

$$\Lambda = H/H_{max}[\Lambda_{min} + \gamma[\Lambda_{max} - \Lambda_{min}]] \qquad \text{(crops and grass)} \tag{59b}$$

Finally, each of the four canopy types is assigned a maximum fractional areal coverage $X_{c,max}$ for each grid square. For trees, the fractional cover X_c at any given time step is taken as equal to $X_{c,max}$. For crops and grass, the effective canopy cover is assumed to be decreased whenever the leaf area index is calculated as falling below 1. In such cases X_c is recalculated as $X_{c,max}\Lambda$, Λ is set back to 1, and an amount $X_{c,max} - X_c$ is added to either the snow-covered or to the bare-soil fraction of the grid square, depending on whether snow cover is present under the canopy or not.

2.6. Implementation in the Canadian Climate Centre GCM

Global data on certain vegetation parameters are required in order to run CLASS in a GCM. From the above discussion, it can be seen that the variables required for each grid square are $\bar{\alpha}_{c,VIS}$, $\bar{\alpha}_{c,NIR}$, $z_{0,max}$, Λ_{max}, Λ_{min}, $W_{c,max}$, $z_{r,max}$, and $X_{c,max}$ for the four major vegetation groups. This information is obtained by making use of the global archive of Wilson and Henderson-Sellers (1985), which contains listings of primary and secondary land covers at a resolution of 1° × 1°. Following a suggestion made in their paper, the 51 land cover types recognized by them are assumed to be characterizable by varying percentages of 24 major categories: e.g. tropical broadleaf tree, long grass, bare soil, glacier ice, etc. On the basis of this information, and assigning a weighting of 75 per cent and 25 per cent to the primary and secondary land cover types respectively, the 24 major categories are obtained at the required GCM grid resolution by performing a weighted average calculation over all of the 1° × 1° squares or parts thereof that fall within each grid square.

If ocean is found to cover more than half of a given grid square, it is assumed to be ocean; if more than half is covered by glacier ice, it is considered as glacier ice. (The latter is treated in effect like bare soil with a possible snow cover, as outlined in Verseghy (1991): the volume fraction of frozen water in the three 'soil' layers is taken to be 1, the thermal properties of ice are used for each layer, and no infiltration of water is allowed at the surface.) To each of the remaining land cover categories, CLASS assigns characteristic values of $X_{c,max}$, $\bar{\alpha}_{c,VIS}$, $\bar{\alpha}_{c,NIR}$, $z_{0,max}$, Λ_{max}, Λ_{min}, $W_{c,max}$, and $z_{r,max}$ (the latter four for vegetation classes only), obtained from the literature. Each land cover category is then assigned to one of five major groups: bare soil, needleleaf trees, broadleaf trees, crops, and grass. (Urban areas are classified as bare soil at present, and are

total fractional snow cover X_s is obtained from equation (35) in Verseghy (1991); the total canopy cover $X_{c,tot}$ is calculated as the sum of the X_c values for the four major canopy types. From these two parameters, the fractional grid square coverages of the four subareas listed above are calculated as $X_{c,tot}X_s$, $X_{c,tot}(1-X_s)$, $(1-X_{c,tot})X_s$, and $(1-X_{c,tot})(1-X_s)$ respectively. The current values of snow albedo and bare soil albedo are determined, and the composite canopy parameters are calculated separately for the canopy covered and canopy-and-snow covered subareas. For each of the four subareas, the energy and moisture fluxes at the canopy, at the ground surface, and between the soil layers are evaluated, the canopy, snow, and soil layer temperatures are updated, and the changes in liquid and frozen moisture stored on the canopy and ground surface and in the soil layers are calculated. Finally, the grid-square average values of the prognostic variables are calculated and stored back into memory.

3. MODEL TESTING AND COMPARISON WITH PREVIOUS SCHEME

Climate simulations were done using two versions of CLASS, in coupled mode with the Canadian Climate Centre (CCC) GCM. In the first version, ponded water remaining on the surface of grid squares at the end of each time step was carried over to the next time step, as described in Verseghy (1991). In the second version, any ponded water that had not infiltrated or evaporated by the end of a given time step was considered to be surface runoff, and was discarded. (This approximates the standard treatment given to ponded water in other GCMs.) These two runs were done in parallel with another one, which featured the old land surface scheme previously used in the GCM (McFarlane *et al.*, 1992). The bare soil model associated with the latter scheme is outlined in Verseghy (1991); where vegetation is present, a few simple modifications are made. For each grid square, the fractional coverage by bare soil, X_g, and the primary and secondary vegetation categories are specified from the data archive of Wilson and Henderson-Sellers (1985). To each of these vegetation categories are assigned characteristic values of visible and near-infrared albedo, snow masking depth, rooting depth, and the 'water use efficiency' parameter; grid-square average values of these terms are calculated by arbitrarily assigning weights of 0·67 and 0·33 to the primary and secondary vegetation categories respectively. The grid-square average albedo is calculated from equation (47) in Verseghy (1991), with α_g replaced by $[X_g\alpha_g+(1-X_g)\alpha_c]$, where α_c is the canopy albedo. The rooting depth is taken as specifying the depth of the 'bucket', and the water use efficiency parameter is incorporated into the calculation of the evaporation efficiency term β (equations (41) and (42) in Verseghy, 1991).

The three runs were all done using the same version of the CCC GCM. This was basically the model described in McFarlane *et al.* (1992), with the addition of some modifications made by Zhang and McFarlane to the parameterization of convection (paper in preparation). A model resolution of T32 was used, with 20 levels in the vertical. FGGE data for 1 January were used to initialize the runs; sea surface temperatures and sea ice extents were prescribed from observations. Each run was integrated for 14 months. Diagnostics were then calculated for the June–July–August season and for the following December–January–February season. In the discussion below, particular attention will be paid to the fields of seasonally averaged screen air temperature and precipitation.

3.1. Results for the June–July–August season

Global observed and modelled average values of screen temperature and precipitation for June, July, and August are presented in Table II. The values of the fields averaged over land surfaces alone are also provided; since sea surface temperatures are prescribed, these give a somewhat clearer picture of the performance of the models. From the information in the table, it can be seen that the old land surface scheme generates a climate that is on the whole too cool and too wet. When land surfaces only are considered, the globally averaged screen temperature is underestimated by 2·7°C, and the global precipitation rate is overestimated by 1·0 mm day^{-1}. The two versions of CLASS, on the other hand, generate climates that are too warm and too wet, but the anomalies are much smaller: 0·2–0·6°C and 0·6–0·7 mm day^{-1} respectively. The climate of the version that retains ponded water is slightly cooler and wetter than that of the version that discards it, because the greater amount of water available at the surface leads to higher evaporation rates.

(b)

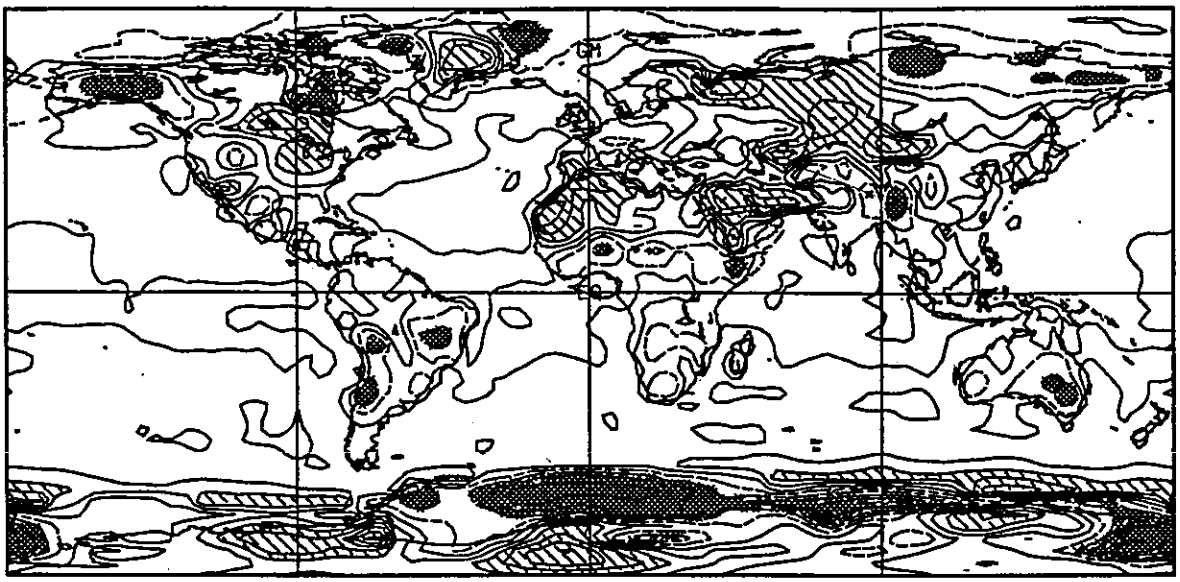

(c)

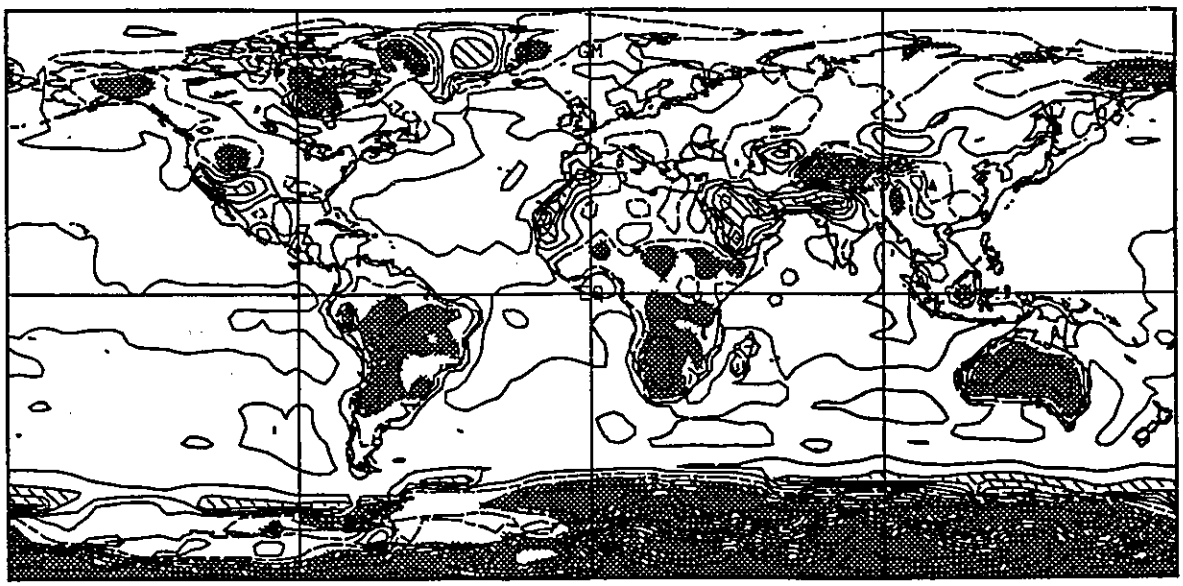

Figure 1. (Continued)

albedo and leaf area index between the dry and wet seasons; such variations are consequently neglected in both CLASS and the old model. The albedo of well-watered vegetation is typically considerably less than that of bare, sandy soil; it is therefore possible that the effective albedo of these areas is being underestimated during the dry season (Northern Hemisphere summer) and overestimated during the wet season. This hypothesis is borne out by the fact that these same areas experience negative screen temperature anomalies in December–January–February (Figure 4).

Another factor that may be contributing to the temperature anomalies observed over deserts in the old scheme is the use of the force-restore method to model the soil thermal regime. This method was developed to

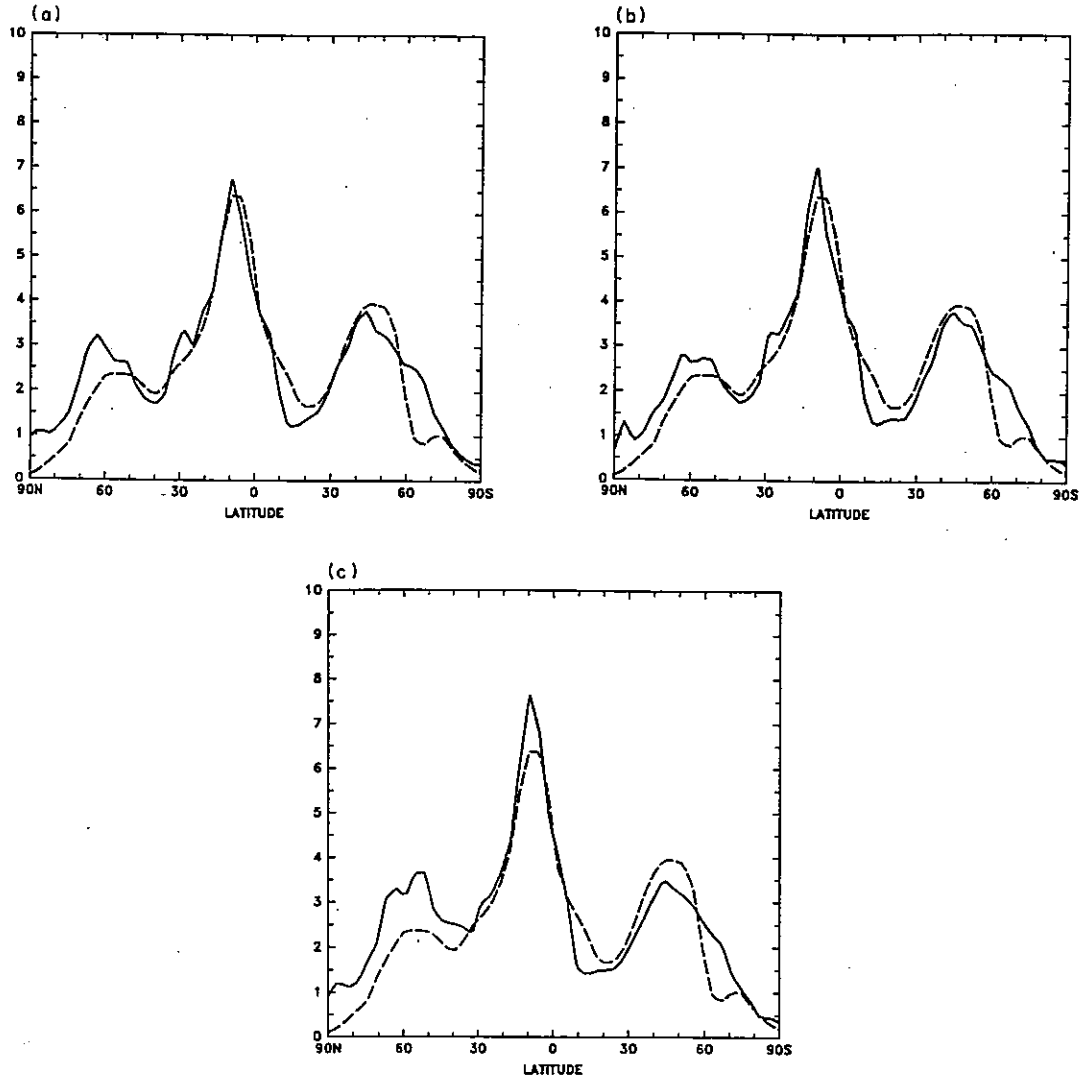

Figure 2. Zonally averaged precipitation rates (mm day^{-1}) for the June–July–August season. Solid lines indicate modelled values, dashed lines observed values. Observations are taken from Jaeger (1976). (a) CLASS: ponded water retained; (b) CLASS: ponded water discarded; (c) old scheme

Looking at the plots of global screen temperature anomalies (Figure 4), it can be seen that there is somewhat more resemblance among the locations and signs of the Northern Hemisphere anomalies generated by the three models than there is in the summer runs. This probably can be attributed to the fact that atmospheric circulations are stronger in the winter, leading to greater persistence of GCM-generated circulation patterns. Measurements taken in remote areas are also likely to be more unreliable in winter, so that some of the observed anomalies may be partly spurious. Large differences in the magnitudes of the anomalies, however, can be assumed to be model-related.

For the old scheme, it is evident that negative anomalies are not quite as widespread as in the season of June–July–August. On the other hand, the magnitudes of anomalies are generally greater. In Northern Hemisphere high latitudes, most of the positive and negative anomalies observed can be attributed to the use of a single layer for soil moisture. The soil thermal model used does not allow surface temperatures to go below 0°C until all of the water in the 'bucket' is frozen. This leads to two results: first, the transition period to

subfreezing surface temperatures is artificially prolonged, and second, once the soil water has frozen completely, the surface temperature plunges quickly to unrealistically low values. (These effects are not observed in CLASS, firstly because surface temperatures are allowed to pass below 0°C before even the first soil layer is entirely frozen, and secondly because the existence of unfrozen lower layers sets up a surfaceward ground heat flux, damping the response of the surface temperature to environmental forcing.) Thus, in very

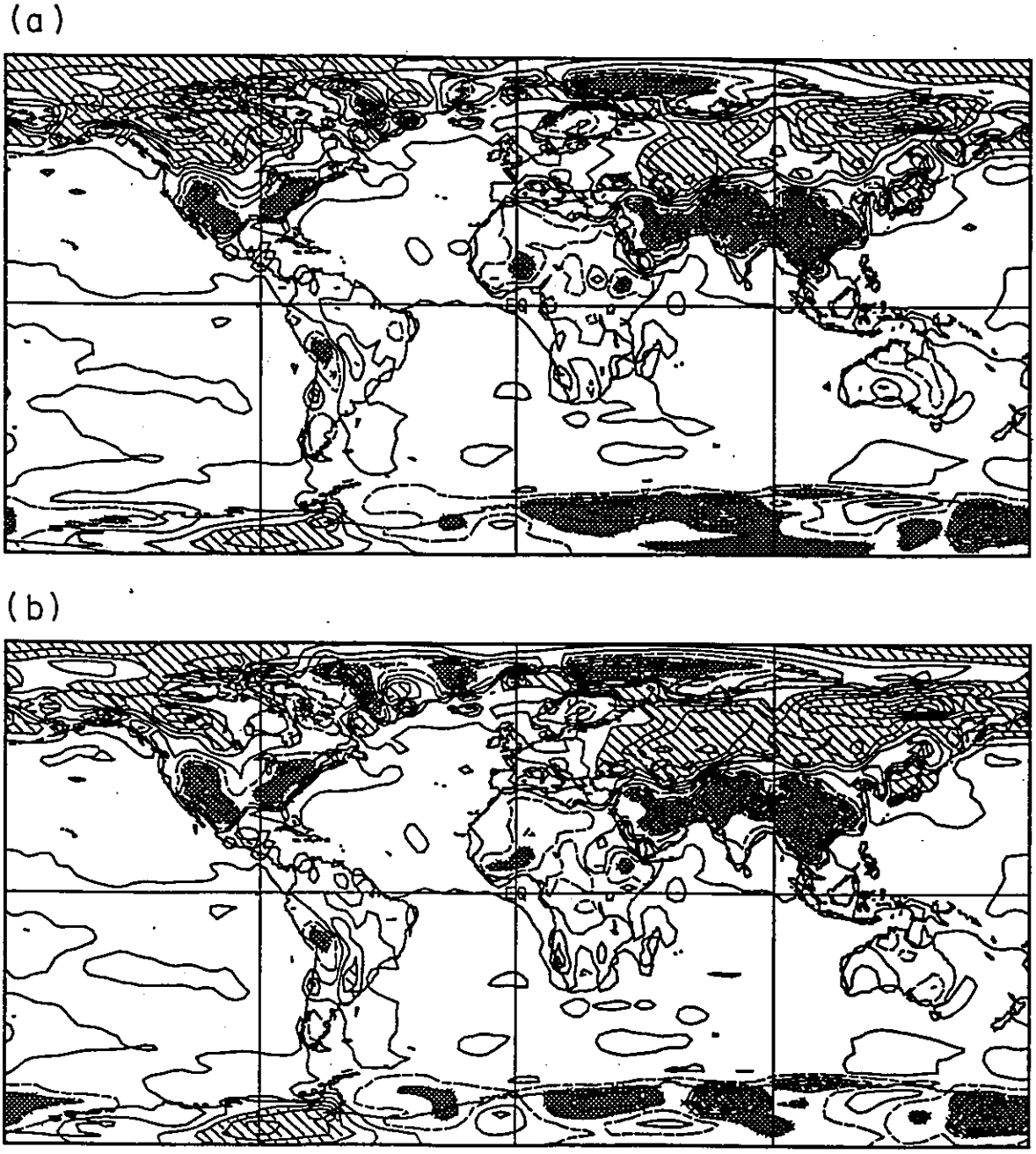

Figure 4. Global screen temperature (°C) anomaly plots (modelled–observed) for the December–January–February season. Diagonal shading indicates values greater than 4°C and cross-hatching values less than −4°C. Contour interval is 2°C; dashed contours indicate negative values. Observed fields were supplied by NCAR. (a) CLASS: ponded water retained; (b) CLASS: ponded water discarded; (c) old scheme

second and third anomalies, while partly explained by the snow masking problem outlined above, are substantially worse in the run in which ponded water is retained. This can be attributed to a problem that arises when the latter version of the model is used in areas underlain by permafrost. In such regions, the surface infiltration and evaporation rates are both very low, with the result that the snow meltwater produced in the spring does not disappear by the following winter. Consequently, when winter arrives this stored water gradually refreezes, releasing latent heat which artificially raises the surface temperature. This problem is currently being circumvented by specifying a maximum ponding depth, but it is clear that some parameterization of surface runoff will have to be developed in the future in order to provide a permanent solution.

In Figure 5, zonally averaged values of precipitation are presented for the three runs and compared with observations. Much the same pattern is evident as in the June–July–August season. The old scheme, as before, generates too much precipitation over the Northern Hemisphere and the tropics, because of its tendency to overestimate land surface evaporation; the magnitude of the Northern Hemisphere anomaly is

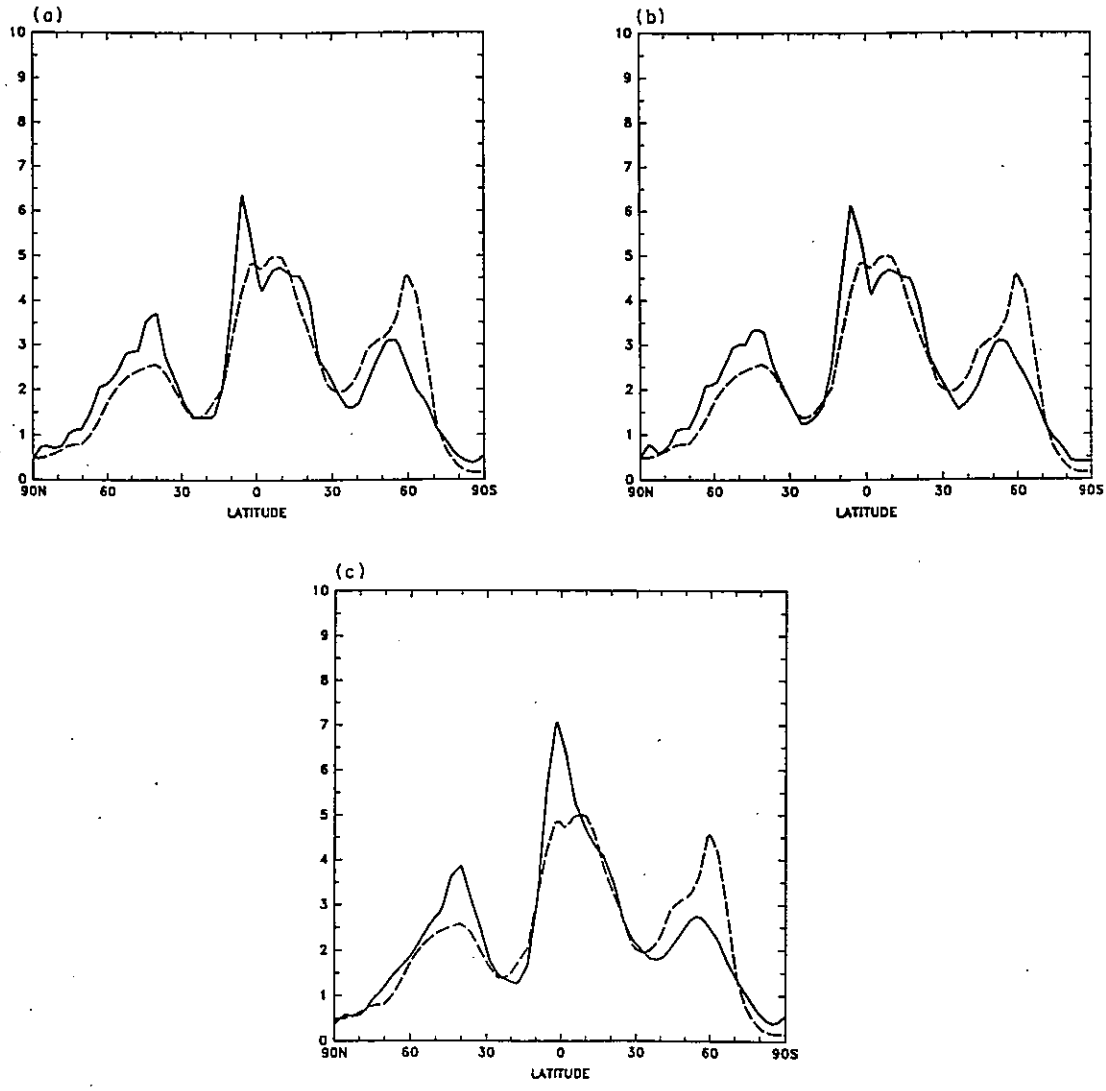

Figure 5. Zonally averaged precipitation rates (mm day^{-1}) for the December–January–February season. Solid lines indicate modelled values, dashed lines observed values. Observations are taken from Jaeger (1976). (a) CLASS: ponded water retained; (b) CLASS: ponded water discarded; (c) old scheme

4. SUMMARY AND CONCLUSIONS

The vegetation model associated with CLASS has been outlined, and its linkages with the soil model introduced in Part I have been described. The strategies used in coupling CLASS to the Canadian Climate Centre GCM have been discussed. The results of a set of test runs have been presented, with the performance of two versions of CLASS being evaluated against that of the older, simpler land surface scheme previously used in the GCM.

The results of the test runs clearly show that the old scheme generates a land surface climate that is considerably too cold and too wet compared with observations. It is argued that in the tropics and in the summer hemisphere, this is primarily caused by the neglect of vegetation stomatal resistances to transpiration. Negative temperature anomalies in winter high latitudes are apparently caused by freezing of the single subsurface soil layer assumed by the bucket model. Summer overestimations and winter underestimations of bare-soil temperatures in desert areas are traced to the neglect of annual-scale forcing from deeper soil layers. (This drawback of the force-restore method was also noted in Verseghy (1991).)

The results generated by CLASS are characterized by considerably smaller temperature and precipitation anomalies. It is postulated that the largest observed screen temperature anomalies are caused by shortcomings in the modelling of the morphological characteristics of vegetation, owing to lack of field data. One of the most important conclusions drawn from this study is that the assumption made in most GCMs that excess surface water is immediately lost to runoff can lead to substantial positive screen temperature anomalies in continental interiors.

A number of improvements still remain to be made to CLASS. Some of these were already recognized in Verseghy (1991). Parameterizations will have to be developed for overland runoff and lateral ground-water flow, particularly in areas underlain by permafrost. Testing of CLASS against the comprehensive data provided by large-scale field experiments, such as HAPEX-MOBILHY, FIFE, BOREAS, etc., will have to be carried out to check and improve parameterizations, particularly those concerned with vegetation characteristics, such as stomatal resistance, snow masking effects, and drought-related variations in albedo and leaf area index. Finally, some ways of improving the modelling of subgrid-scale variability of convective precipitation and surface soil moisture may have to be sought: perhaps along the lines of the work of Warrilow *et al.* (1986), Wetzel and Chang (1988) and Entekhabi and Eagleson (1989). The division of each grid square into four subareas admittedly provides no more than a first approximation to the solution of this problem. Despite the fledgling state of CLASS, however, the present study clearly indicates that it provides a much more realistic simulation of land surface climates than does a simple 'force-restore *cum* bucket' type of model.

REFERENCES

Abramopoulos, F., Rosenzweig, C. and Choudhury, B. 1988. 'Improved ground hydrology calculations for global climate models (GCMs): Soil water movement and evapotranspiration', *J. Climate*, **1**, 921–941.

Avissar, R., Avissar, P., Mahrer, Y. and Bravdo, B. A. 1985. 'A model to simulate response of plant stomata to environmental conditions', *Agric. For. Meteorol.*, **34**, 21–29.

Avissar, R. and Pielke, R. A. 1989. 'A parameterization of heterogeneous land surfaces for atmospheric numerical models and its impact on regional meteorology', *Mon. Wea. Rev.*, **117**, 2113–2136.

Brutsaert, W. 1979. 'Heat and mass transfer to and from surfaces with dense vegetation or similar permeable roughness', *Boundary-Layer Meteorol.*, **16**, 365–388.

Carlson, T. N., Perry, E. M. and Schmugge, T. J. 1990. 'Remote estimation of soil moisture availability and fractional vegetation cover for agricultural fields', *Agric. For. Meteorol.*, **52**, 45–69.

Carson, D. J. 1986. *Parametrizations of Land-suface Processes in Meteorological Office Numerical Weather Prediction and Climate Models*, Meteorological Office, Bracknell, DCTN 37, 54 pp.

Deardorff, J. W. 1972. 'Parameterization of the planetary boundary layer for use in general circulation models', *Mon. Wea. Rev.*, **100**, 93–106.

Deardorff, J. W. 1978. 'Effective prediction of ground surface temperature and moisture, with inclusion of a layer of vegetation', *J. Geophys. Res.*, **83**(C4), 1889–1903.

Dickinson, R. E., Henderson-Sellers, A., Kennedy, P. J. and Wilson, M. F. 1986. *Biosphere–Atmosphere Transfer Scheme (BATS) for the NCAR Community Climate Model*, National Centre for Atmospheric Research, Boulder, Colorado, NCAR/TN-275+STR, 69 pp.

Entekhabi, D. and Eagleson, P. S. 1989. 'Land surface hydrology parameterization for atmospheric general circulation models including subgrid scale variability', *J. Climate*, **2**, 816–831.